TECHNICAL NOTES

NATIONAL ADVISORY COMMITTEE FOR AERONAUTICS

No. 582

ANALYSIS AND MODEL TESTS OF AUTOGIRO JUMP TAKE-OFF

By John B. Wheatley and Carlton Bioletti
Langley Memorial Aeronautical Laboratory

Washington
October 1936

NATIONAL ADVISORY COMMITTEE FOR AERONAUTICS

TECHNICAL NOTE NO. 582

ANALYSIS AND MODEL TESTS OF AUTOGIRO JUMP TAKE-OFF

By John B. Wheatley and Carlton Bioletti

SUMMARY

An analysis is made of the autogiro jump take-off, in which the kinetic energy of the rotor turning at excess speed is used to effect a vertical take-off. By the use of suitable approximations, the differential equation of motion of the rotor during this maneuver is reduced to a form that can be solved. Only the vertical jump was studied; the effect of a forward motion during the jump is discussed briefly. The results of model tests of the jump take-off have been incorporated in the paper and used to establish the relative accuracy of the results predicted from the analysis. Good agreement between calculation and experiment was obtained by making justifiable allowances.

INTRODUCTION

One of the recent developments of the autogiro is the maneuver variously described as the "jump take-off," "direct take-off," and "jump-off." This maneuver, hereafter referred to as the "jump take-off," is a take-off with a flight path initially vertical, effected by the release of excess kinetic energy stored in the rotor. The energy is stored by driving the rotor at a speed greater than its normal speed in flight, and during this process the pitch of the rotor blades is reduced to zero. The driving mechanism is disconnected when the desired speed has been attained, the rotor pitch is suddenly increased to either its normal value or a higher one, and the consequent thrust, which is greater than the weight of the machine, lifts it vertically from the ground. During the jump, the rotor decelerates, and the propeller must be operated at full throttle so that the forward speed of the machine will be at least equal to its minimum speed in level flight by the time that the rotor speed drops to its normal value. At this same time, if a rotor pitch greater than normal has been employed for the jump, this high

pitch must be reduced to normal. The machine now continues flight from the top of the jump as if a conventional take-off had just been completed.

The jump take-off promises two important advantages: first, take-off becomes independent of the type of ground available insofar as mud, roughness, or high grass is concerned; and second, the machine is enabled to clear much higher obstacles in a given distance and thus can operate from more restricted fields.

The possibilities of the jump take-off have been established by some full-scale experiments. It is the purpose of this paper to study the factors that govern the jump take-off in its simplest form and to present the results of model tests in which the effect of differences in the rotor parameters was determined.

ANALYSIS

In order to simplify the analysis, it will be assumed that during the jump the forward velocity of the machine is zero. The justifications of such an assumption are: first, that the height of jump so obtained will represent a lower limit to the heights attained in practice where forward velocities of varying magnitudes will reduce the induced power losses in the rotor; and second, the actual magnitudes of the forward velocities attained will vary with wind velocity, thrust-weight ratio, and piloting technique and consequently cannot be generalized even for a single set of values of the rotor parameters.

The thrust T of a rotor at a tip-speed ratio of zero is, from reference 1,

$$T = \frac{1}{2} \rho \Omega^2 \pi R^4 \sigma a \left\{ \frac{1}{2} \lambda B^2 + \frac{1}{3} \theta_o B^3 + \frac{1}{4} \theta_1 B^4 \right\} \quad (1)$$

where ρ, air density, slug/cu. ft.

Ω, rotor angular velocity, rad./sec.

R, rotor radius, ft.

λ, axial-flow coefficient.

θ_o, rotor pitch angle at hub, radians.

θ_1, difference between rotor pitch angles at hub and at tip, radians.

B, factor multiplying radius to allow for tip losses.

σ, rotor solidity, for rectangular blades equal to number of blades b times blade chord c divided by πR; $\sigma = \frac{bc}{\pi R}$.

a, slope of lift curve of rotor blade airfoil section in radian measure.

Similarly, the rotor torque Q is

$$Q = \frac{1}{2} \rho \Omega^2 \pi R^5 \sigma a \left\{ \frac{1}{2} \lambda^2 B^2 + \frac{1}{3} \lambda \theta_o B^3 + \frac{1}{4} \lambda \theta_1 B^4 - \frac{\delta}{4a} \right\} \quad (2)$$

where δ is the mean rotor blade profile-drag coefficient. Inspection shows that, if $C_T = \frac{T}{\rho \Omega^2 \pi R^4}$ and $C_Q = \frac{Q}{\rho \Omega^2 \pi R^5}$,

$$C_Q = \lambda C_T - \frac{1}{8} \sigma \delta \quad (3)$$

The axial flow $\lambda \Omega R$ is expressed as follows:

$$\lambda \Omega R = - v - \dot{h} \quad (4)$$

where v, rotor induced velocity, ft./sec.

$\dot{h}$, rotor vertical velocity, ft./sec.

From the momentum theory, as in reference 1, when the tip-speed ratio is zero,

$$v = \frac{T}{2\rho \pi R^2 \sqrt{(V')^2}} = \frac{\frac{1}{2} C_T \Omega R}{+\sqrt{\lambda^2}} \quad (5)$$

where V' = resultant velocity of rotor, ft./sec., and is equal to $- v - \dot{h} = \lambda \Omega R$. Equation (5) is written in such a way as to show that the induced velocity v is independ-

ent of the sign of λ; but since λ is always negative during the jump,

$$\lambda = \frac{\frac{1}{2} C_T}{\lambda} - \frac{\dot{h}}{\Omega R} \qquad (6)$$

Substitute for C_T from (1); then

$$\lambda^2 + \lambda \left(\frac{\dot{h}}{\Omega R} - \frac{1}{8} \sigma a B^2\right) - \frac{1}{12} \sigma a \theta_0 B^3 - \frac{1}{16} \sigma a \theta_1 B^4 = 0 \qquad (7)$$

and $$\lambda = \frac{1}{16} \sigma a B^2 - \frac{1}{2} \frac{\dot{h}}{\Omega R} - \left\{\left(\frac{1}{16} \sigma a B^2 - \frac{1}{2} \frac{\dot{h}}{\Omega R}\right)^2 + \frac{1}{12} \sigma a \theta_0 B^3 + \frac{1}{16} \sigma a \theta_1 B^4\right\}^{\frac{1}{2}} \qquad (8)$$

The equations for λ, C_T, and C_Q now make possible the justification of a necessary approximation. On figures 1 and 2 are shown the variation of C_Q with the vertical velocity ratio $\dot{h}/\Omega R$ for a series of values of θ_0, with θ_1 always zero. The computation was made for $\sigma = 0.05$ on figure 1 and for $\sigma = .10$ on figure 2. It is proposed that C_Q be assumed independent of $\dot{h}/\Omega R$; this approximation is seen to be reasonable on figure 1 for the lower values of $\dot{h}/\Omega R$ at all pitches less than 16°; the error introduced by the approximation is greater in figure 2 where the solidity is 0.10 but is still reasonably small for the lower values of $\dot{h}/\Omega R$. Experimental justification for this assumption will subsequently be presented.

If C_Q is assumed constant during the jump, it becomes possible to obtain the instantaneous angular velocity of the rotor as a function of known constants. Then

$$I \dot{\Omega} = Q = \rho \Omega^2 \pi R^5 C_Q \qquad (9)$$

where $\dot{\Omega}$, angular acceleration, rad./sec.^{2}.

I, mass moment of inertia of rotor about axis of rotation, slug-ft.^{2}

t, time, sec.

Segregating variables and integrating

$$-\frac{1}{\Omega} = \frac{\rho \pi R^5}{I} C_Q t + C_1 \tag{10}$$

Letting the time be zero at the beginning of the jump, and designating the initial rotor angular velocity as Ω_o,

$$C_1 = -\frac{1}{\Omega_o} \tag{11}$$

and

$$\Omega = \frac{\Omega_o}{1 + \frac{\rho \pi R^5}{I} \Omega_o C_Q t} \tag{12}$$

Now let the total weight to be lifted by the rotor be W; then

$$\frac{W}{g} \ddot{h} = T - W \tag{13}$$

where $\ddot{h}$ is the vertical acceleration of rotor, ft./sec.^{2}. The thrust T is given in (1) as a function of Ω, λ, and the physical constants of the rotor. However, λ is a function of $\dot{h}$ and Ω, as seen in (8), so equation (8) will now be examined. The radical in (8) can be expanded by the binomial theorem; then

$$\lambda = \frac{1}{16} \sigma a B^2 - \frac{1}{2} \frac{\dot{h}}{\Omega R} - \left\{\frac{1}{12} \sigma a \theta_o B^3 + \frac{1}{16} \sigma a \theta_1 B^4\right\}^{\frac{1}{2}} - \frac{\frac{1}{512} \sigma^2 a^2 B^4 - \frac{1}{32} \sigma a B^2 \frac{\dot{h}}{\Omega R} + \frac{1}{8} \frac{\dot{h}^2}{\Omega^2 R^2}}{\left\{\frac{1}{12} \sigma a \theta_o B^3 + \frac{1}{16} \sigma a \theta_1 B^4\right\}^{\frac{1}{2}}} + \ldots \tag{14}$$

In figures 3 and 4 are presented values of λ as functions of $\dot{h}/\Omega R$ for several values of the pitch angle θ_o; the calculation was based on a solidity of 0.05 in figure 3 and on a solidity of 0.10 in figure 4. Two methods of calculating λ were employed. First, λ was calculated directly from (8) and, second, the first three terms of equation (14) were used. The agreement between the exact expression and the approximation is considered satisfactory for values of $\dot{h}/\Omega R$ less than 0.07; it will later be shown that the discrepancy is of such a character as to perhaps be desirable. It will consequently be assumed

that the first three terms of (14) constitute a satisfactory expression for λ.

Substitute for λ from (14) in (1); the rotor thrust T becomes

$$T = \frac{1}{2}\rho\Omega^2\pi R^4 \sigma a \left\{\frac{1}{32}\sigma a B^4 - \frac{1}{4}B^2\frac{\dot{h}}{\Omega R} - \frac{1}{2}B^2\left(\frac{1}{12}\sigma a\theta_0 B^3 + \frac{1}{16}\sigma a\theta_1 B^4\right)^{\frac{1}{2}} + \frac{1}{3}\theta_0 B^3 + \frac{1}{4}\theta_1 B^4\right\} \quad (15)$$

The final substitution required is that for Ω from (12); then

$$T = \frac{\frac{1}{2}\rho\Omega_0^2\pi R^4\sigma a}{\left(1 - \frac{\rho\pi R^5}{I}\Omega_0 C_Q t\right)^2}\left\{\frac{1}{32}\sigma a B^4 - \frac{1}{2}B^2\left(\frac{1}{12}\sigma a B^3\theta_0 + \frac{1}{16}\sigma a B^4\theta_1\right)^{\frac{1}{2}} + \frac{1}{3}\theta B^3 + \frac{1}{4}\theta_1 B^4\right\} - \frac{\frac{1}{8}\rho\Omega_0\pi R^3\sigma a B^2}{\left(1 - \frac{\rho\pi R^5}{I}\Omega_0 C_Q t\right)}\dot{h} \quad (16)$$

This expression can be abbreviated by designating the initial value of the thrust coefficient as C_{T_0}, which is

$$C_{T_0} = \frac{1}{2}\sigma a\left\{\frac{1}{32}\sigma a B^4 - \frac{1}{2}B^2\left(\frac{1}{12}\sigma a\theta_0 B^3 + \frac{1}{16}\sigma a\theta_1 B^4\right)^{\frac{1}{2}} + \frac{1}{3}\theta_0 B^3 + \frac{1}{4}\theta_1 B^4\right\} \quad (17)$$

Then T becomes

$$T = \frac{\rho\Omega_0^2\pi R^4 C_{T_0}}{\left(1 - \frac{\rho\pi R^5}{I}\Omega_0 C_Q t\right)^2} - \frac{1}{8}\frac{\rho\Omega_0\pi R^3\sigma a B^2}{\left(1 - \frac{\rho\pi R^5}{I}\Omega_0 C_Q t\right)}\dot{h} \quad (18)$$

The expression for T in (18) may now be substituted in (13), giving

$$\ddot{h} = \frac{g}{W}\frac{\rho\Omega_0^2\pi R^4 C_{T_0}}{\left(1 - \frac{\rho\pi R^5}{I}\Omega_0 C_Q t\right)^2} - \frac{1}{8}\frac{g}{W}\frac{\rho\Omega_0\pi R^3\sigma a B^2}{\left(1 - \frac{\rho\pi R^5}{I}\Omega_0 C_Q t\right)}\dot{h} - g \quad (19)$$

Let $$K_1 = \frac{1}{8}\frac{g}{W}\rho\,\Omega_0\,\pi\,R^3\,\sigma\,a\,B^2 \qquad (20)$$

$$K_2 = -\frac{\rho\,\pi\,R^5}{I}\Omega_0\,C_Q \qquad (21)$$

$$K_3 = \frac{g}{W}\rho\,\Omega_0^2\,\pi\,R^4\,C_{T_0} = g\frac{T_e}{W} \qquad (22)$$

Then

$$\ddot{h} + \frac{K_1}{1 + K_2 t}\dot{h} = \frac{K_3}{(1 + K_2 t)^2} - g \qquad (23)$$

This expression is seen to be a linear differential equation in $\dot{h}$ which can be integrated quite simply. Reference to a text on differential equations establishes that the solution of (23) is

$$\dot{h}\,(1+K_2t)^{\frac{K_1}{K_2}} = \frac{K_3}{K_1-K_2}(1+K_2t)^{\frac{K_1}{K_2}-1} - \frac{g}{K_1+K_2}(1+K_2t)^{\frac{K_1}{K_2}+1} + C_1 \qquad (24)$$

By transposition

$$\dot{h} = \frac{K_3}{(K_1-K_2)\,(1+K_2t)} - \frac{g\,(1+K_2t)}{K_1+K_2} + \frac{C_1}{(1+K_2t)^{\frac{K_1}{K_2}}} \qquad (25)$$

The constant C_1 is evaluated by substituting the values $\dot{h} = 0$ at $t = 0$; then

$$C_1 = \frac{g\,(K_1-K_2) - K_3\,(K_1+K_2)}{(K_1^2 - K_2^2)} \qquad (26)$$

Consequently

$$\dot{h} = \frac{K_3}{(K_1-K_2)\,(1+K_2t)} - \frac{g(1+K_2t)}{K_1+K_2} + \frac{g\,(K_1-K_2)-K_3(K_1+K_2)}{(K_1^2-K_2^2)\,(1+K_2t)^{\frac{K_1}{K_2}}} \qquad (27)$$

Equation (27) thus expresses the vertical velocity $\dot{h}$ during the rise in terms of the time t and the known constants of the rotor K_1, K_2, and K_3. By direct differentiation and integration of (27), the net vertical accel-

eration $\ddot{h}$ and the height h can be obtained. Then

$$\ddot{h} = \frac{-K_2K_3}{(K_1-K_2)\ (1+K_2t)^2} - \frac{gK_2}{K_1+K_2} - \frac{gK_1(K_1-K_2)-K_1K_3(K_1+K_2)}{(K_1^2-K_2^2)\ (1+K_2t)^{1+\frac{K_1}{K_2}}} \quad (28)$$

And

$$h = \frac{K_3}{K_2(K_1-K_2)} \log\ (1+K_2t) - \frac{g(t+\frac{1}{2}\ K_2t^2)}{K_1+K_2}$$

$$- \frac{g(K_1-K_2)-K_3(K_1+K_2)}{(K_1-K_2)\ (K_1^2-K_2^2)\ (1+K_2t)^{\frac{K_1}{K_2}-1}} + C_2 \quad (29)$$

The constant C_2 is evaluated as before by setting $h = 0$ when $t = 0$;

$$C_2 = \frac{g\ (K_1-K_2) - K_3\ (K_1+K_2)}{(K_1-K_2)\ (K_1^2-K_2^2)} \quad (30)$$

The resultant expression for h is

$$h = \frac{K_3}{K_2(K_1-K_2)} \log\ (1+K_2t) - \frac{g(t+\frac{1}{2}\ K_2t^2)}{K_1+K_2}$$

$$- \frac{g(K_1-K_2)-K_3(K_1+K_2)}{(K_1-K_2)(K_1^2-K_2^2)(1+K_2t)^{\frac{K_1}{K_2}-1}} + \frac{g(K_1-K_2)-K_3(K_1+K_2)}{(K_1-K_2)(K_1^2-K_2^2)} \quad (31)$$

Equations (27), (28), and (31) constitute the complete solution of the equations of motion of the autogiro during a jump take-off. The known factors required for the solution are the physical characteristics of the rotor, comprising the radius R, the solidity σ, the lift-curve slope a, the gross weight W, the moment of inertia I, the pitch angle θ_0, and the initial speed Ω_0. From these items the constants K_1, K_2, and K_3 are derived, and the acceleration, vertical velocity, and vertical displacement can then be determined.

The physical significance of the constants K_1, K_2, and K_3 (equations (20), (21), and (22)) may assist in

obtaining a clear understanding of the analysis. The constant K_1 represents the amount by which a vertical velocity $\dot{h}$ of 1 ft./sec. would reduce the ratio of rotor thrust to the mass being lifted at the beginning of the jump take-off. This factor occurs in the differential equation of motion divided by $(1 + K_2 t)$, where K_2 is a factor determining the rotor speed as a function of time (see equation (12)). The constant K_3 is quite simply equal to the ratio of the initial thrust to weight, multiplied by g, the acceleration of gravity. It is consequently apparent that K_3 must always exceed g in order that a jump be obtained. In addition, the smaller K_1 and K_2 are for a given value of K_3, the greater will be the jump; and the greater K_3 is with K_1 and K_2 fixed, the greater will be the jump.

The alteration in the jump take-off that will be effected by a forward velocity during the jump will be almost entirely caused by the change in λ and consequently in the induced losses in the rotor arising from a value of $\mu = \frac{V \cos \alpha}{\Omega R}$ different from zero. The expression for λ becomes, when μ is not zero,

$$\lambda = \frac{-\frac{1}{2} C_T}{\sqrt{\mu^2 + \lambda^2}} - \frac{\dot{h}}{\Omega R} \qquad (32)$$

and C_T and C_Q both become dependent upon μ to some extent. If μ never increases above 0.1, and the minimum speed in level flight usually corresponds to less than that value, the change in the expressions for C_T and C_Q can be neglected as a first approximation, and the solution of the equation of motion can be obtained step by step by considering only λ to be a function of μ. Equation (32) shows that λ increases algebraically as μ increases, which means that C_T will be greater and C_Q a smaller negative value under that condition. It is consequently obvious that an increase in μ will increase the thrust and decrease the simultaneous loss of kinetic energy in the rotor, resulting in a greater jump. The step-by-step solution of the jump take-off with forward velocity has not been made, because the value of the results to be obtained was considered incommensurate with the labor required. It is of interest that the time required for an

existing autogiro to attain a forward speed of 25 miles per hour during a jump take-off is of the order of 2 seconds; this represents the minimum time that should elapse before the vertical velocity reaches zero at the end of the jump take-off for this particular machine.

EXPERIMENTAL INVESTIGATION

Apparatus and Tests

The model rotor used in the jump take-off tests had the following physical characteristics:

Radius	5 ft.
Blade chord	0.523 ft.
Solidity	0.10
Moment of inertia (total)	3.23 slug-ft.^{2}
Airfoil section	N.A.C.A. 0018

The pitch of the rotor blades was adjustable on the ground but was fixed at a constant value while the rotor was being brought up to speed and jumped.

The tests were conducted in the return passage of the full-scale wind tunnel, which provided an enclosed space about 50 feet by 200 feet, 70 feet high. The apparatus used in the tests is shown diagrammatically in figure 5. The model rotor A supported the ballast B; the rotor was driven by a 25-horsepower electric motor C through a pair of bevel gears inside the box D. A means was provided for restraining the rotor from rising until a catch was released by remote manual control. Cables E were attached to the rotor and rose with it as it jumped; the cables passed over pulleys near the roof and were wound upon the drum F, which was actuated by the counterweight G. The diameters of the drum F and the pulley to which the counterweight was attached were in the ratio of 10:1, so that neglecting friction the cable tension would be 0.1 times the weight of the counterweight. The drum F was restrained from rotation by a ratchet except in such a direction as to wind up the cables E; this device prevented the model from falling after the completion of a jump.

A time history of the height of jump was obtained by attaching a cord to the bottom of the model and recording the displacement of the cord, through a reduction mechanism, on an N.A.C.A. control-position recorder fastened to the frame that served as a base for the motor and driving mechanism. The rotor speed during a jump was measured by photographing the rotor with a motion-picture camera placed beneath the rotor with its lens axis vertical; time was recorded on each frame by photographing simultaneously a sweep hand rotating at one revolution per second. The resultant time history of rotor revolutions yielded the rotor speed and angular acceleration by two successive graphical differentiations. A typical camera record is shown in figure 6. Initial rotor speeds were, in addition, observed on an electric tachometer connected to a magneto driven by the shaft which in turn rotated the model.

The tests made were of such a scope as to provide information on the effect of pitch angle, initial rotor speed, and disk loading upon the height of jump. Since it was necessary to maintain a small tension in the cables E (fig. 4), tests were also made at fixed values of the three primary variables but with varying amounts of cable tension, provided by changing the weight of the counterweight G. Tests were made with pitch angles of from 6° to 18°, with disk loadings of from 0.46 to 1.66 pounds per square foot, and with initial rotor speeds of from 450 to 725 r.p.m. The initial rotor speed was limited in some cases at large pitch angles because the motor power was insufficient to increase the speed further; in other cases, the limiting rotor speed was that at which the height of jump reached 20 feet to 25 feet, which was considered as high as was desirable.

Results

The results of the model tests are presented in tables I and II showing the maximum height attained by the rotor as a function of the pitch angle, disk loading, initial rotor speed, and cable tension; the cable tension T_c as tabulated is equal to 0.1 times the counterweight. Table I includes all data taken without measuring the rotor speed with the motion-picture camera; the data in table II were obtained while the camera was being used.

The form into which the data were transformed is illustrated in figures 7 and 8, which show, respectively, the curves of height and rotor revolutions with their first

and second time derivatives. All differentiations were performed graphically.

The camera data are plotted in figure 9 in the form of $1/\Omega$ against time, where $1/\Omega$ is chosen as the dependent variable because the slope of the resultant curve is a direct measure of the rotor torque coefficient. Table III presents a comparison of the measured and calculated values of C_Q.

In order to check the analysis, calculations of several jumps were made employing the constants of the model rotor. Since the influence of the cable tension on the jumps was uncertain, the calculations were made for several model weights equal to and less than the actual model weight as an approximation of the influence of the cable tension. The results of these calculations are presented in figures 10, 11, 12, and 13.

Precision

The experimental curves of height against time were obtained within limits of ± 0.2 foot at a given time. The graphical differentiation of the resultant curve unfortunately depends to a large extent upon the fairing of the height curve, so that the vertical-velocity curves may be in error by as much as ± 1 foot per second. The records of rotor displacement against time could be read to within $\pm 2^\circ$ of angular displacement; the angular-velocity curves, because of graphical differentiation, are less accurate and probably are in error by as much as ± 0.5 revolution per second.

Other sources of error in the experimental work are almost negligible. The rotor pitch angle was adjusted to within $\pm 0.1^\circ$ at rest and, since the rotor blade section was symmetrical and was balanced about the quarter-chord point, the dynamic twist should have been small. Any error in the remaining physical constants of the model can be neglected.

DISCUSSION

The introduction of approximations into the solution of the equations for the jump take-off requires consideration of the errors introduced in order to estimate the validity of the final results. The two principal approxi-

mations used are that the torque coefficient C_Q be independent of the vertical velocity and that the axial-flow coefficient λ can be satisfactorily expressed by using only the first term of the expansion of the radical in the exact expression.

The data in figures 1 and 2 demonstrate that the assumption of constant C_Q is reasonable for the smaller values of $\dot{h}/\Omega R$; in addition, figure 9 verifies the assumption experimentally for the case of $\sigma = 0.10$, since the curves of $1/\Omega$ against time depart but a small amount from straight lines. Figures 1 and 2 demonstrate that the greater the solidity, the greater will be the departure of C_Q from a constant value. However, considerations other than the jump take-off dictate that full-scale solidities will approach 0.05; for such solidities, the errors introduced by the assumption of constant C_Q appear to be negligible.

The approximation to λ in which all terms but the first of the binomial expansion of the radical were neglected, introduces an error demonstrated in figures 3 and 4. It will be seen that the approximate λ is always algebraically greater than the exact λ. This condition is not undesirable, because the jump take-off will always be made in proximity to the ground plane, and "ground-effect" will reduce the rotor induced velocity and consequently change λ in the same direction as the approximation. Unfortunately, the variation of the induced velocity with distance from the rotor has not been established, so that the actual magnitude of the ground effect cannot be estimated; the effect is undoubtedly important while the rotor is less than one diameter from the ground, and the resultant change in λ is probably greater than the error introduced by the approximation. It is thought that these considerations justify this approximation as well as the first, and that the approximation to λ introduces no serious error in the analysis.

When applying the analysis, it is desirable to calculate the rotor speed from equation (12) as a function of time and to use this as a check on the height of rise. If the rotor speed drops to its normal value before the vertical velocity is zero, the height at this time should be regarded as the maximum attainable, rather than the height at which the vertical velocity is zero with the rotor speed below normal. This conclusion follows from the con-

sideration that the transition to normal flight must not be hampered by the necessity to increase the rotor speed, since such a requirement would probably result in a momentary loss of height.

The validity of the analysis is attested by figures 10, 11, 12, and 13. The figures establish that the allowance that should be made for the cable tension is considerably less than the nominal value of this variable, which is a reasonable result considering the effects of friction and the acceleration of the cable and drum by the counterweight. Figures 10 and 11 show close agreement when the allowances for cable tension are 10 pounds and 15 pounds, respectively; the nominal values of the tension were 12.5 pounds and 17.5 pounds. The general form of the height and velocity curves in both figures agrees quite closely with experiment. Figures 12 and 13 illustrate the same points as figures 10 and 11, except that a smaller allowance for the same cable tension results in agreement; the allowances indicated are approximately 3 pounds and 7 pounds for the 12.5-pound and 17.5-pound cable tension. These values are rather small, and indicate that the analysis is not as exact at a pitch angle of 18° as at one of 10°.

It will be noted in table III that the experimental and calculated torque coefficients differ by an appreciable amount. The ratio of the calculated to the experimental value is between 0.81 and 0.86; the difference between the measured and calculated torques at a pitch of 14° and a rotor speed of 600 r.p.m. is 14 pound-feet. This value is considerably greater than could be accounted for by bearing friction. The fact that the torque coefficient is in error at the same time that reasonable agreement is obtained on the height and velocity records indicates the existence of a compensating error. It is considered possible that the source of this compensating error is the ground effect, which would tend to increase the thrust of the rotor when it was near the ground plane at no additional cost in torque. Another possibility is that the rotor pitch angle increased slightly because of the dynamic twist of the rotor blades; while this twist should be quite small, a twist of approximately 1° would explain most of the discrepancies between the torque coefficients of table III.

Because of the limitations encountered during the model tests, it is unlikely that the experimental results

obtained will be directly applicable in design. They have served a useful purpose in attesting the validity of the mathematical analysis, which can be used with more confidence than would have been justified without experimental verification.

The principal uses of the analysis will be: the prediction of the lower limits of the jump take-off for given values of the physical constants of the rotor; the prediction of the effect of changes in the rotor to obtain higher jumps; and the establishment of the form of the height and velocity curves for jumps at constant pitch angles.

Langley Memorial Aeronautical Laboratory,
National Advisory Committee for Aeronautics,
Langley Field, Va., August 7, 1936.

REFERENCE

1. Wheatley, John B.: An Aerodynamic Analysis of the Autogiro Rotor with a Comparison between Calculated and Experimental Results. T.R. No. 487, N.A.C.A., 1934.

TABLE I

Pitch angle θ_o, deg.	Disk loading $\frac{W}{\pi R^2}$ lb./sq.ft.	Initial rotor speed N_o, r. p. m.	Cable tension (approx.) T_o, lb.	Maximum height H_{max}, ft	Pitch angle θ_o, deg.	Disk loading $\frac{W}{\pi R^2}$ lb./sq.ft.	Initial rotor speed N_o, r. p. m.	Cable tension (approx.) T_o, lb.	Maximum height H_{max}, ft	Pitch angle θ_o, deg.	Disk loading $\frac{W}{\pi R^2}$ lb./sq.ft.	Initial rotor speed N_o, r. p. m.	Cable tension (approx.) T_o, lb.	Maximum height H_{max}, ft.
6	0.46	650	12.5	22.6	10	.76	550	17.5	17.9	12	1.66	700	17.5	8.2
6	.46	654	12.5	21.3	10	.76	552	17.5	17.4	12	1.66	698	17.5	8.4
6	.46	654	7.5	15.8	10	.76	552	12.5	15.1	12	1.66	698	12.5	7.0
6	.46	602	7.5	9.0	10	.76	550	12.5	14.0	12	1.66	696	12.5	7.0
6	.46	602	7.5	9.7	10	.76	499	12.5	7.7	12	1.66	693	17.5	7.9
6	.76	724	12.5	7.6	10	.76	499	12.5	7.7	12	1.66	695	17.5	7.9
6	.76	726	12.5	7.9	10	.76	495	17.5	10.0	14	1.66	687	17.5	10.2
6	.76	724	7.5	6.2	10	.76	497	17.5	10.0	14	1.66	693	17.5	10.0
6	.76	724	7.5	7.2	10	.76	479	17.5	8.0	16	1.66	700	17.5	13.0
8	.76	724	12.5	25.5	10	.76	479	17.5	7.7	16	1.66	702	17.5	12.8
8	.76	700	12.5	22.4	10	.76	479	12.5	6.3	16	1.66	648	17.5	9.5
8	.76	700	12.5	22.6	10	.76	479	12.5	6.2	16	1.66	650	17.5	9.7
8	.76	700	17.5	27.0	10	.76	550	12.5	14.8	18	1.66	655	17.5	11.5
8	.76	698	17.5	27.6	10	.76	550	12.5	14.6	18	1.66	648	17.5	11.0
8	.76	646	17.5	20.5	10	.76	550	17.5	19.0	18	1.66	600	17.5	7.7
8	.76	648	17.5	20.8	10	.76	550	17.5	18.7	18	1.66	599	17.5	7.4
8	.76	650	12.5	16.8	10	.76	600	17.5	26.8	18	1.66	600	12.5	6.9
8	.76	650	12.5	17.9	10	.76	600	17.5	27.6	18	1.66	600	12.5	7.1
8	.76	598	12.5	11.5	10	.76	600	12.5	23.4	18	1.66	550	12.5	3.3
8	.76	602	12.5	11.7	10	.76	600	12.5	22.4	18	1.66	550	12.5	3.2
8	.76	598	7.5	8.8	10	1.06	700	12.5	16.9	18	1.66	550	17.5	3.5
8	.76	598	7.5	8.8	10	1.06	700	12.5	17.4	18	1.66	555	17.5	4.2
8	1.06	724	12.5	10.8	10	1.06	700	17.5	19.8	18	1.66	550	17.5	3.8
8	.76	598	17.5	14.7	10	1.06	700	17.5	19.8	18	1.36	550	17.5	9.0
8	.76	600	17.5	14.3	10	1.06	655	17.5	15.6	18	1.36	543	17.5	8.2
8	.76	550	17.5	8.2	10	1.06	600	17.5	9.4	18	1.36	550	12.5	8.2
8	.76	550	17.5	8.0	10	1.06	603	17.5	9.4	18	1.36	550	12.5	7.4
8	.76	552	12.5	4.2	10	1.06	600	12.5	7.9	18	1.36	600	17.5	13.8
8	.76	549	12.5	5.6	10	1.06	598	12.5	8.2	18	1.36	600	17.5	13.8
8	.76	550	12.5	5.5	10	1.06	550	17.5	4.5	18	1.36	500	17.5	4.6
8	.76	561	7.5	4.8	10	1.06	547	17.5	4.6	18	1.36	500	17.5	4.4
8	.76	580	7.5	6.8	10	1.06	550	12.5	3.3	18	1.36	500	12.5	3.5
8	.76	580	7.5	6.9	10	1.06	550	12.5	3.8	18	1.36	500	12.5	4.0
8	.76	558	7.5	4.6	10	1.06	550	12.5	3.7	18	1.36	491	12.5	3.4
8	.76	561	7.5	5.0	10	1.06	652	12.5	12.0					
8	1.06	725	12.5	3.4	10	1.06	650	12.5	12.0					
8	.46	549	17.5	37.7	10	1.06	652	17.5	14.6					
8	.46	550	17.5	38.2	10	1.06	650	17.5	14.3					
8	.46	497	17.5	26.3	10	1.06	700	17.5	19.0					
8	.46	499	17.5	27.9	10	1.06	700	17.5	19.5					
8	.46	497	12.5	19.8	10	1.06	700	12.5	17.3					
8	.46	499	12.5	19.5	10	1.06	700	12.5	17.7					
8	.46	449	12.5	10.7	10	1.36	700	12.5	7.5					
8	.46	449	12.5	11.0	10	1.66	735	12.5	5.4					
8	.46	445	17.5	16.6	10	1.66	700	12.5	3.9					
8	.46	451	17.5	17.4	10	1.66	700	12.5	3.7					
					10	1.66	700	17.5	4.2					
					10	1.66	702	17.5	4.5					

TABLE II

Pitch angle θ_o, deg.	Disk loading $\frac{W}{\pi R^2}$ lb./sq.ft.	Initial rotor speed N_o, r.p.m.	Cable tension (approx.) T_c, lb.	Maximum height H_{max}, ft.
10	1.36	700	17.5	9.2
10	1.36	650	17.5	6.3
10	1.36	600	17.5	2.6
10	1.66	700	17.5	4.5
10	1.66	700	17.5	4.2
14	1.36	650	17.5	14.6
14	1.36	600	17.5	9.9
14	1.36	599	17.5	9.5
14	1.36	549	17.5	5.0
14	1.36	550	17.5	5.2
14	1.66	647	17.5	7.0
14	1.66	599	17.5	4.0
14	1.66	600	17.5	5.0
14	1.66	600	17.5	4.8
14	1.66	650	17.5	7.9
18	1.06	500	17.5	11.0
18	1.06	500	17.5	11.3
18	1.06	550	17.5	17.7
18	1.06	550	17.5	16.6
18	1.36	550	17.5	9.2
18	1.36	550	17.5	9.2
18	1.36	497	17.5	5.0
18	1.36	500	17.5	3.8
18	1.36	600	17.5	13.5
18	1.36	600	17.5	14.0
18	1.66	550	17.5	4.1
18	1.66	550	17.5	3.8
18	1.66	597	17.5	7.7
18	1.66	603	17.5	7.7
18	1.66	647	17.5	10.4
18	1.66	647	17.5	10.2

TABLE III

Pitch angle θ_o, deg.	$\frac{d\left(\frac{1}{\Omega}\right)}{dt}$ $\frac{\text{sec./rad.}}{\text{sec.}}$	Meas. C_Q	Calc. C_Q
10	0.00525	-0.000726	-0.000587
14	.00812	-.001122	-.000969
18	.01273	-.001760	-.001460

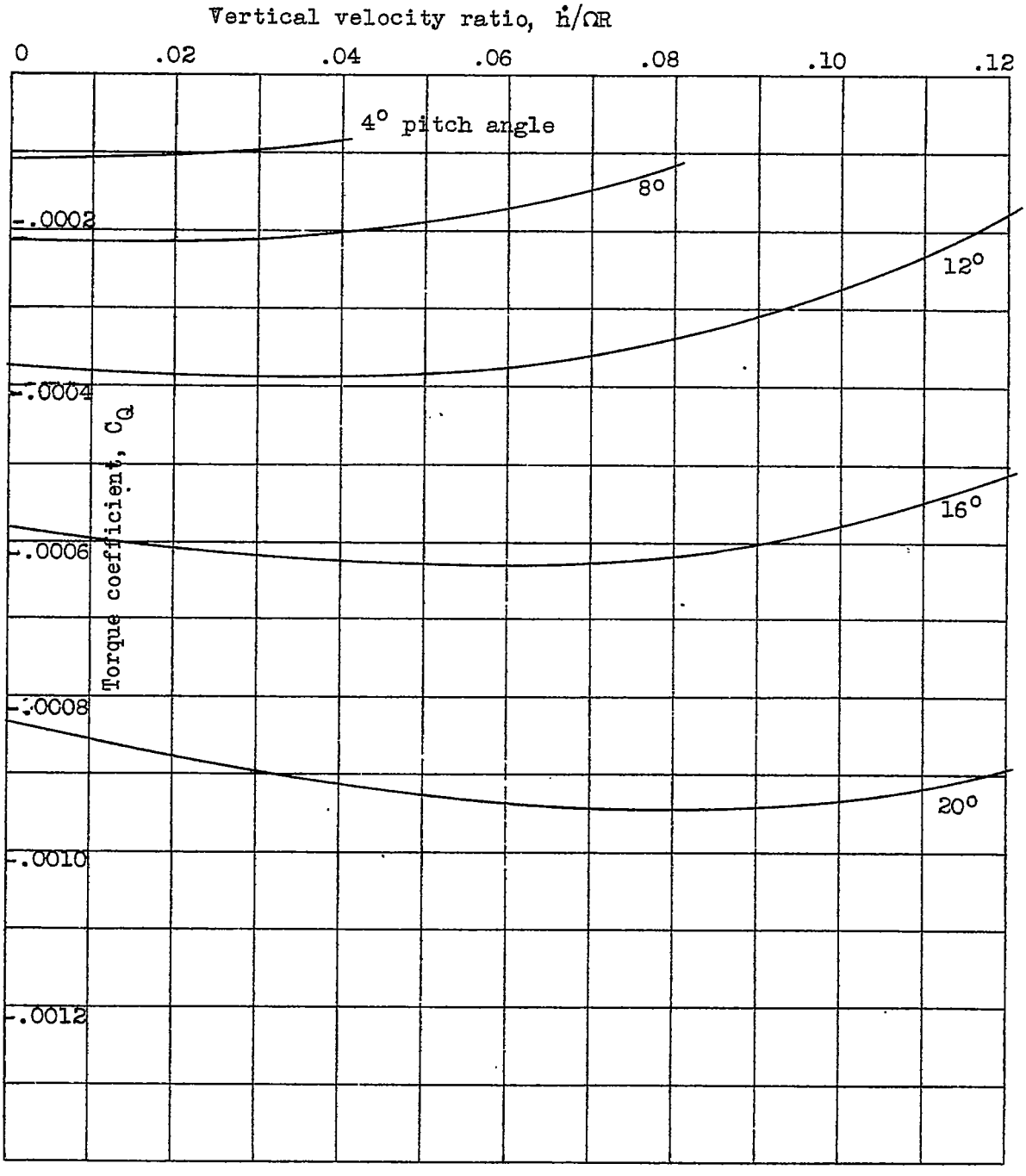

Figure 1.- Calculated torque coefficient C_Q as a function of the vertical velocity ratio $\dot{h}/\Omega R$ for several pitch angles. $\sigma = 0.05$.

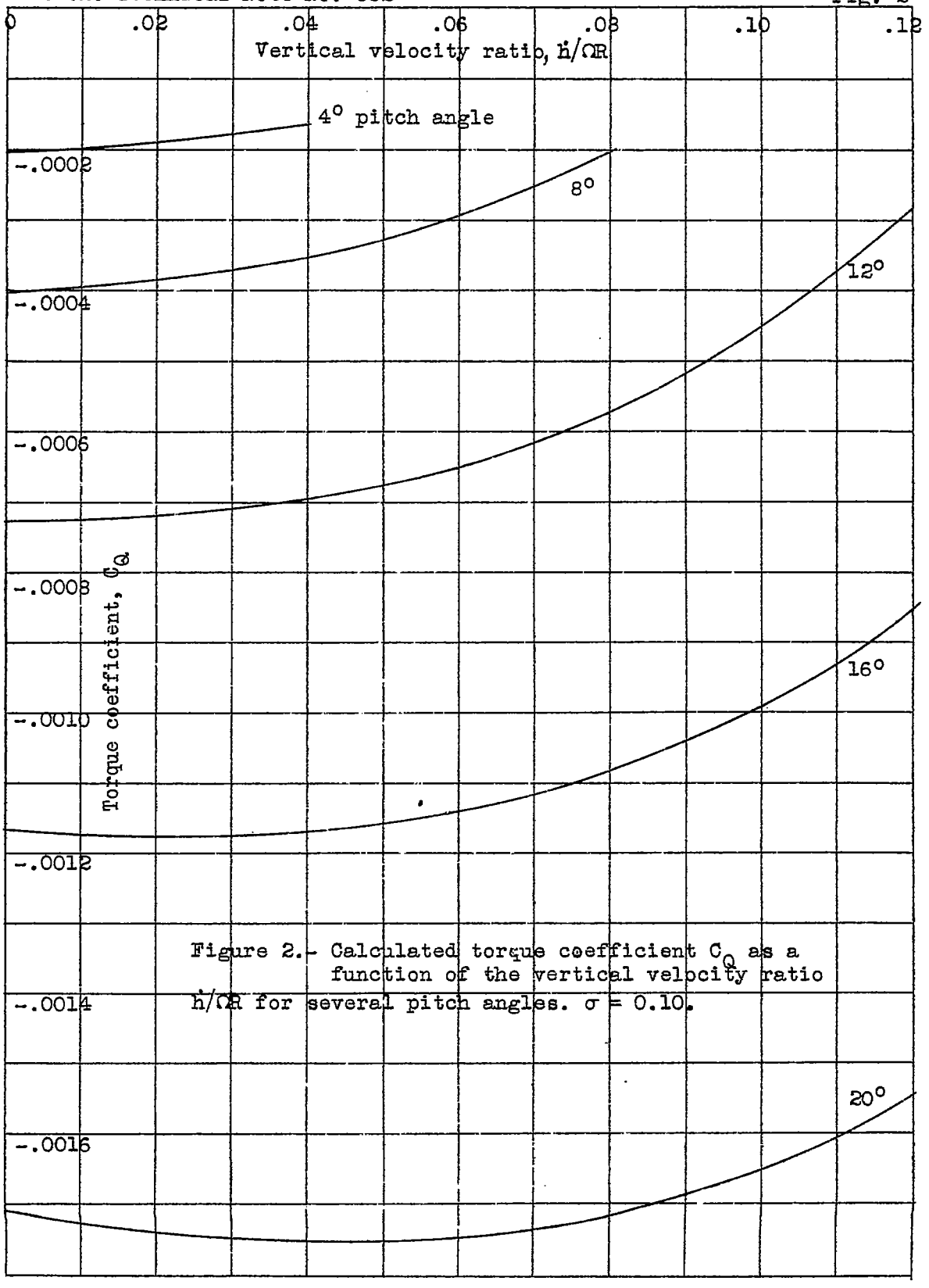

Figure 2.- Calculated torque coefficient C_Q as a function of the vertical velocity ratio $\dot{h}/\Omega R$ for several pitch angles. $\sigma = 0.10$.

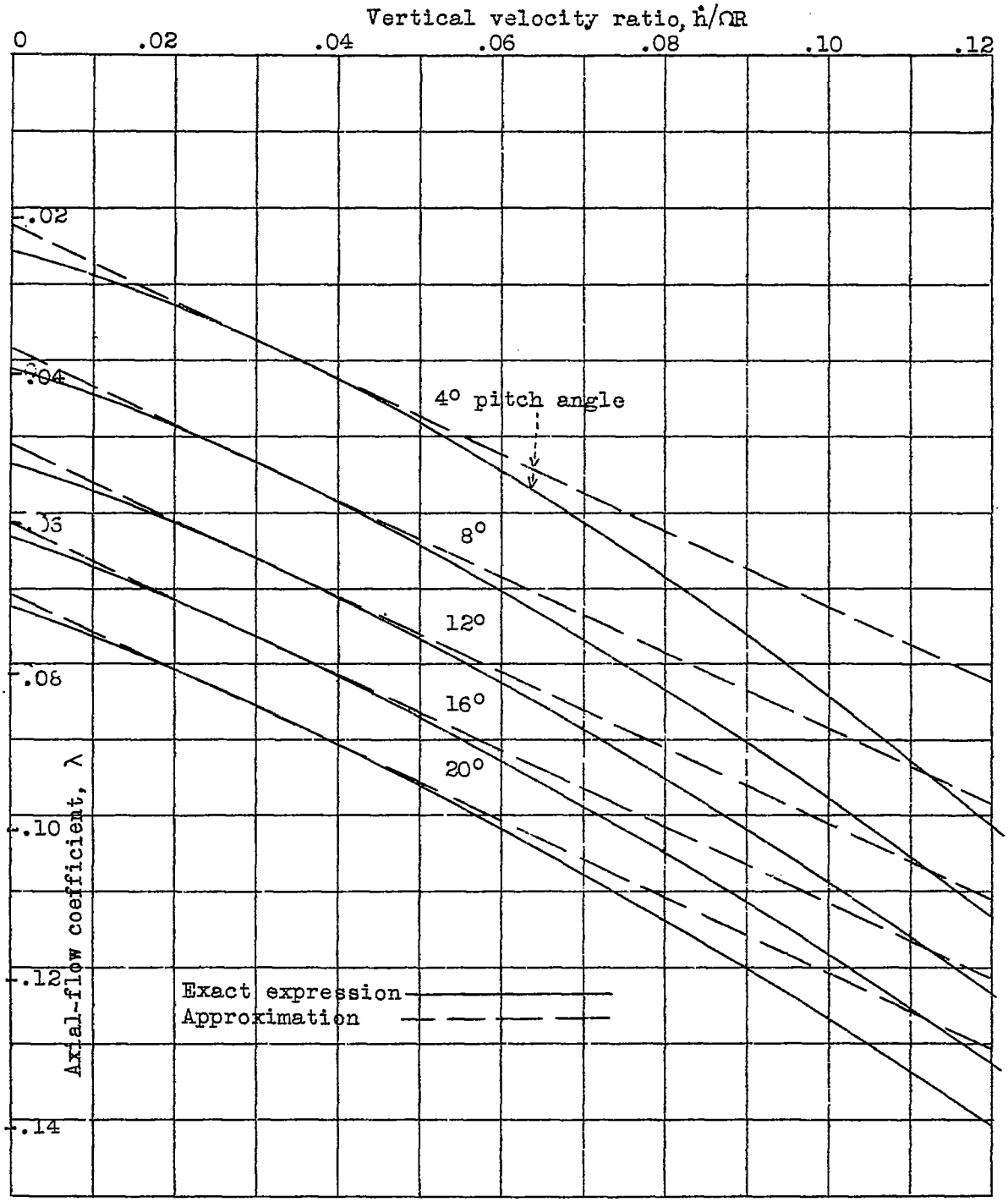

Figure 3.- Calculated axial-flow coefficient λ as a function of the vertical velocity ratio $\dot{h}/\Omega R$ for several pitch angles - exact and approximate solutions. $\sigma = 0.05$.

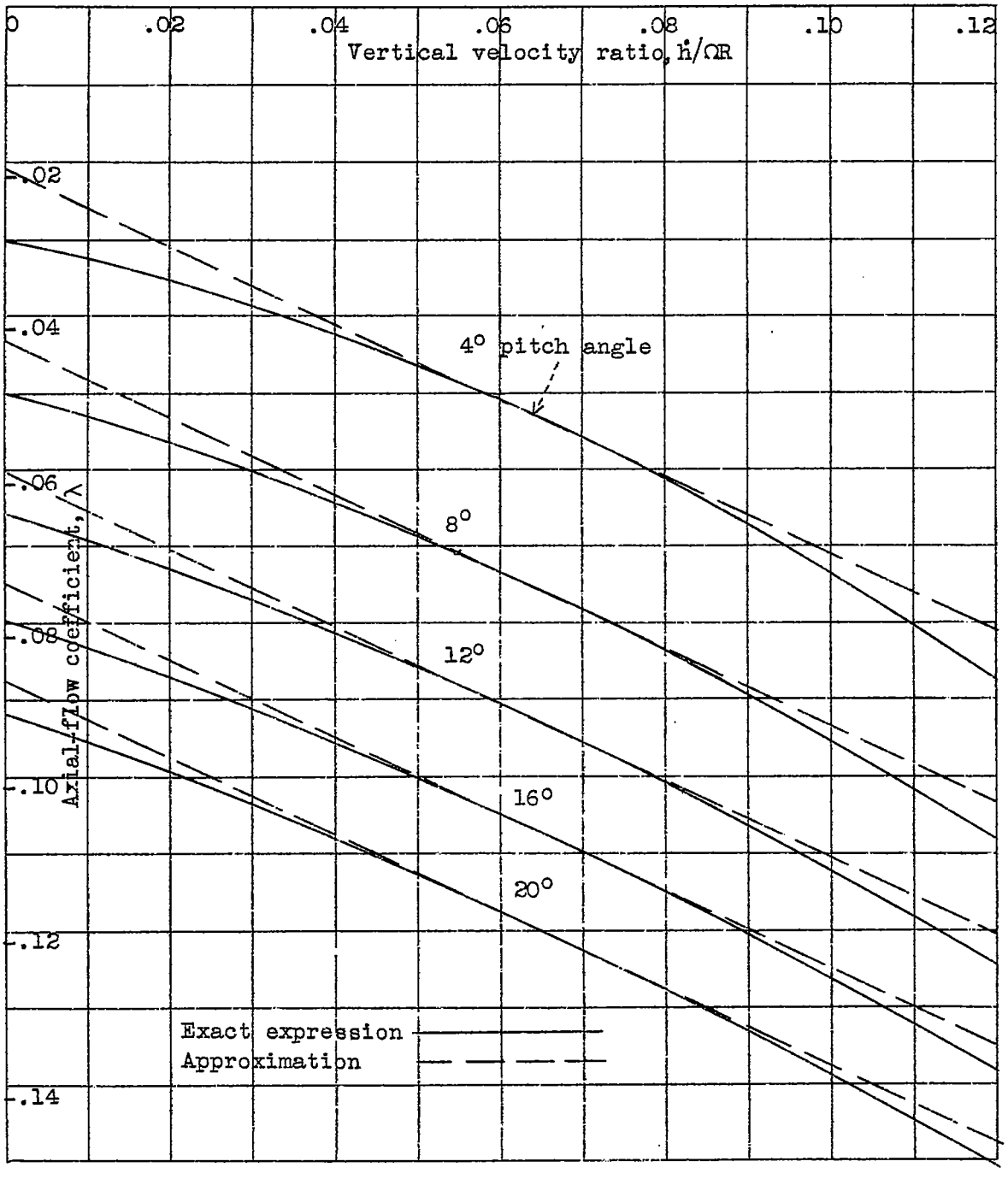

Figure 4.- Calculated axial-flow coefficient λ as a function of the vertical velocity ratio $\dot{h}/\Omega R$ for several pitch angles-exact and approximate solutions. $\sigma = 0.10$.

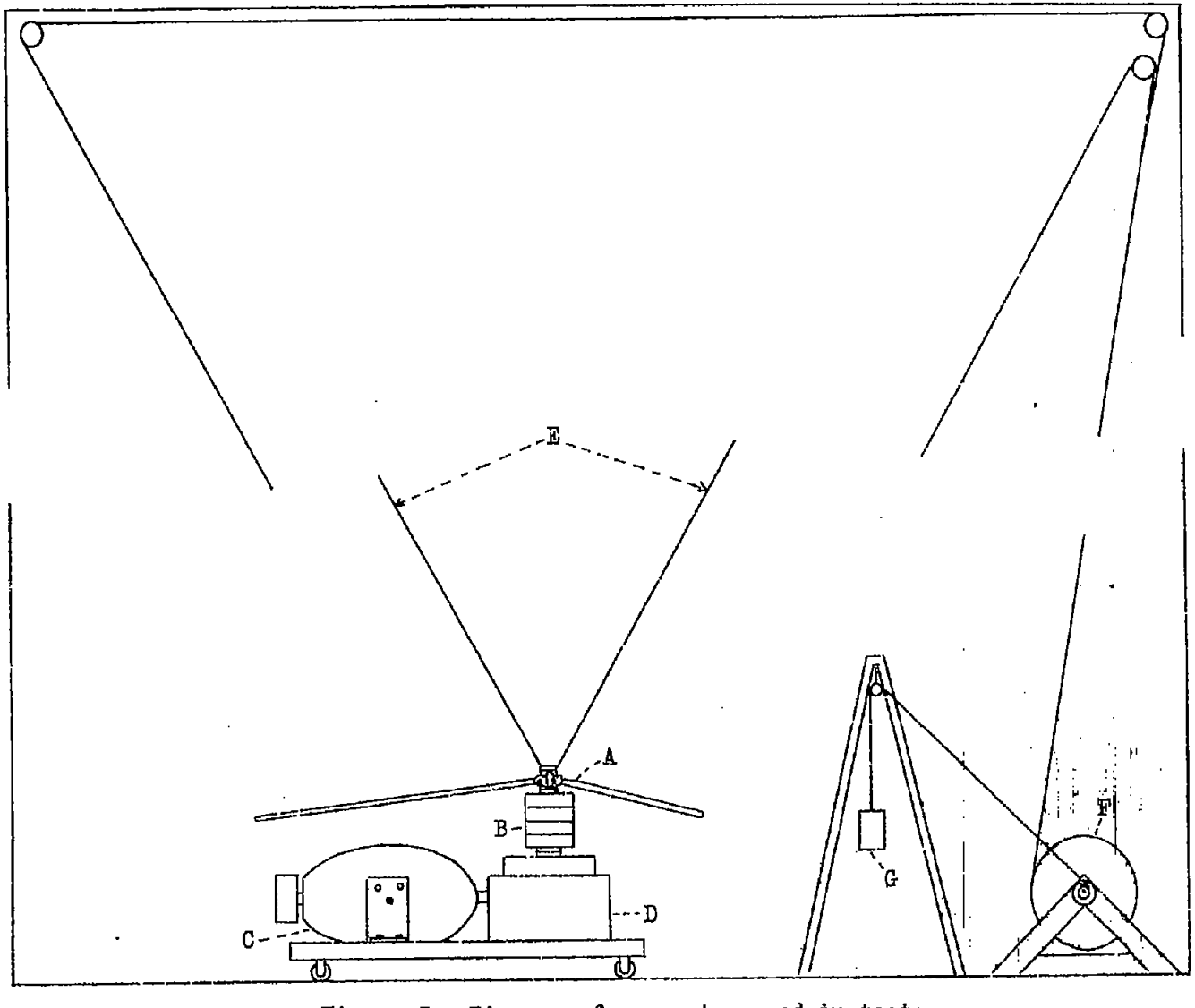

Figure 5.- Diagram of apparatus used in tests.

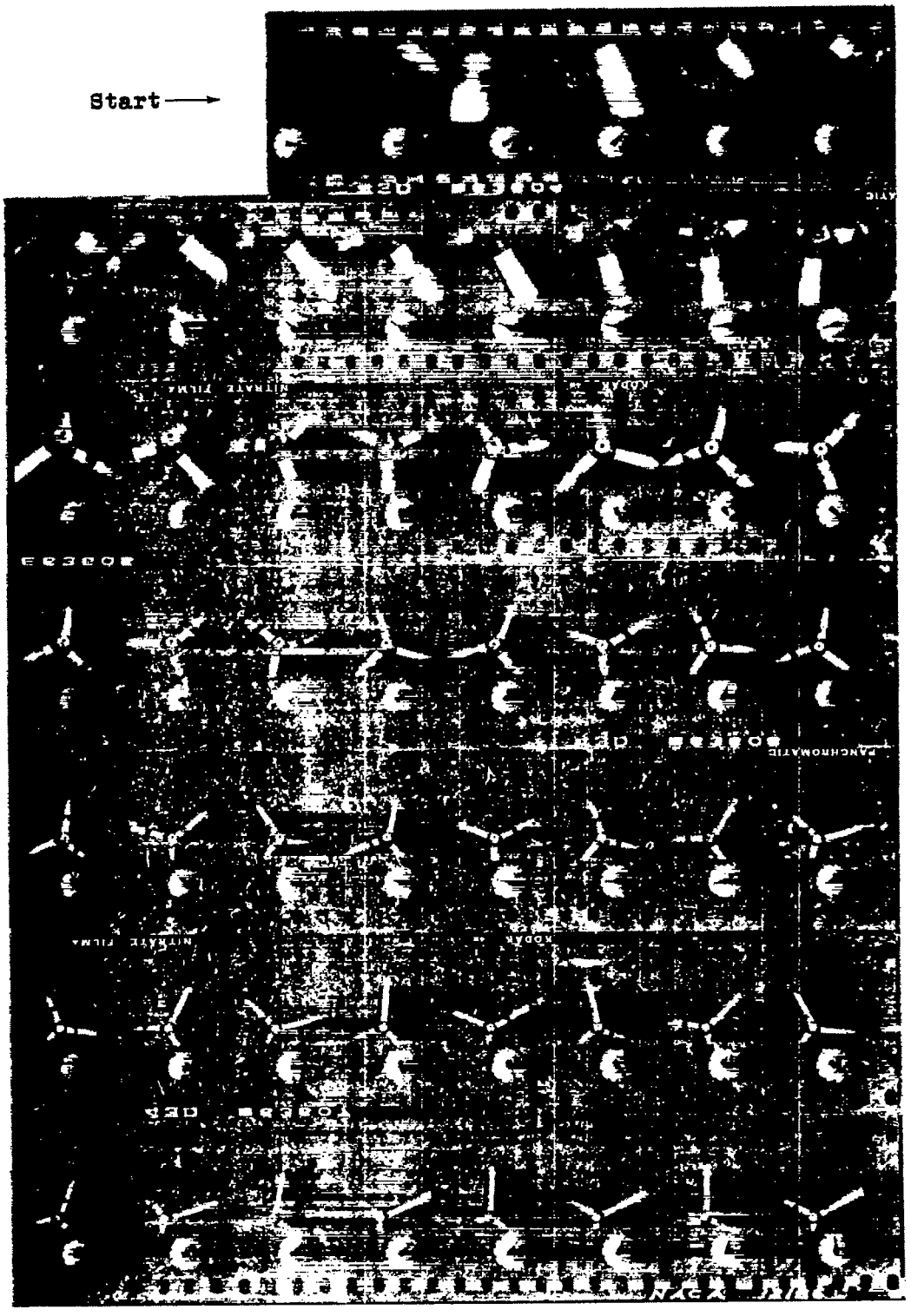

Figure 6.- Sample test record of rotor displacement, speed, and acceleration against time.

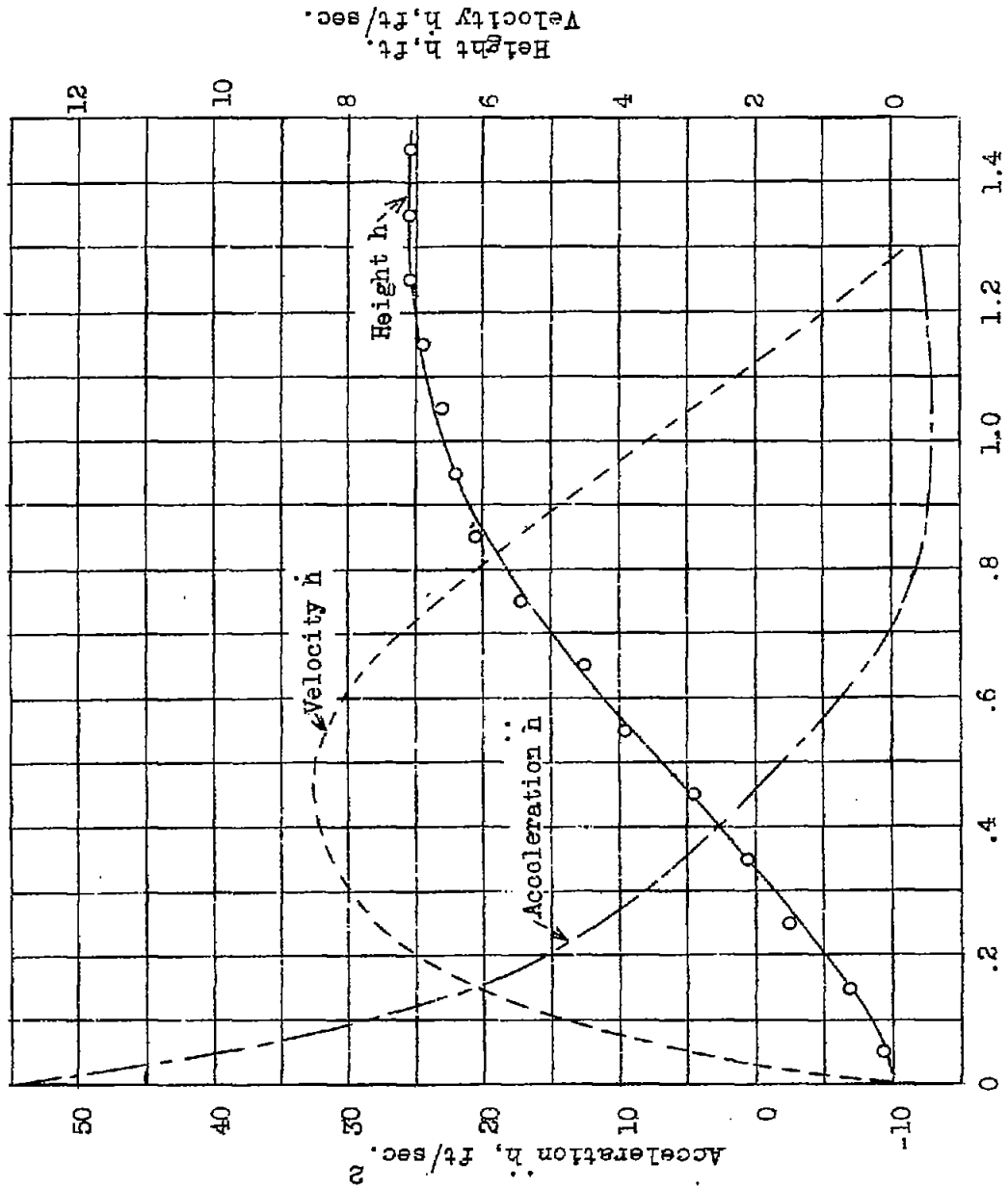

Figure 7.- Typical height, vertical velocity, and vertical acceleration work-up of test record.

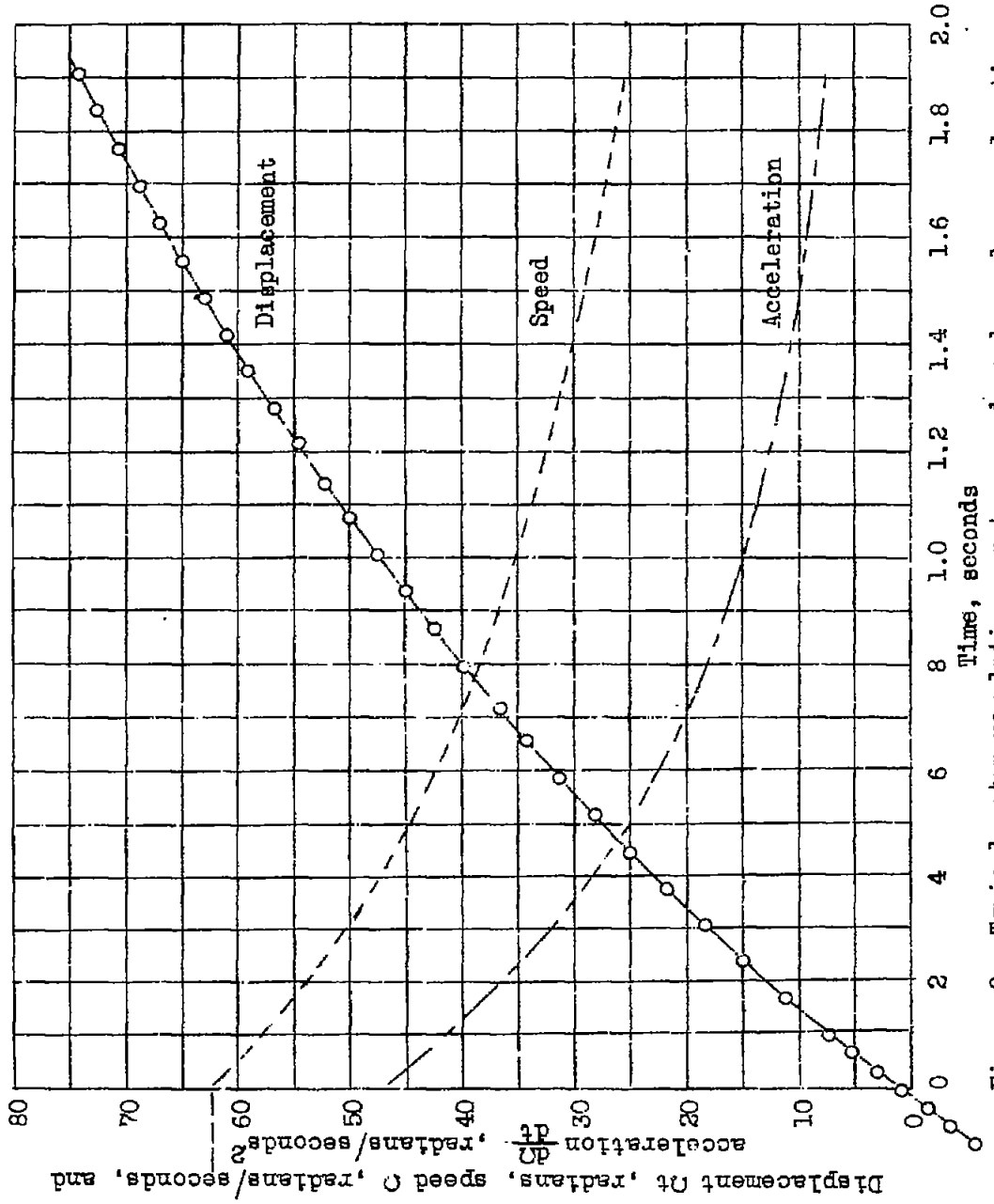

Figure 8.- Typical rotor revolutions, rotor speed, and angular acceleration work-up of test record.

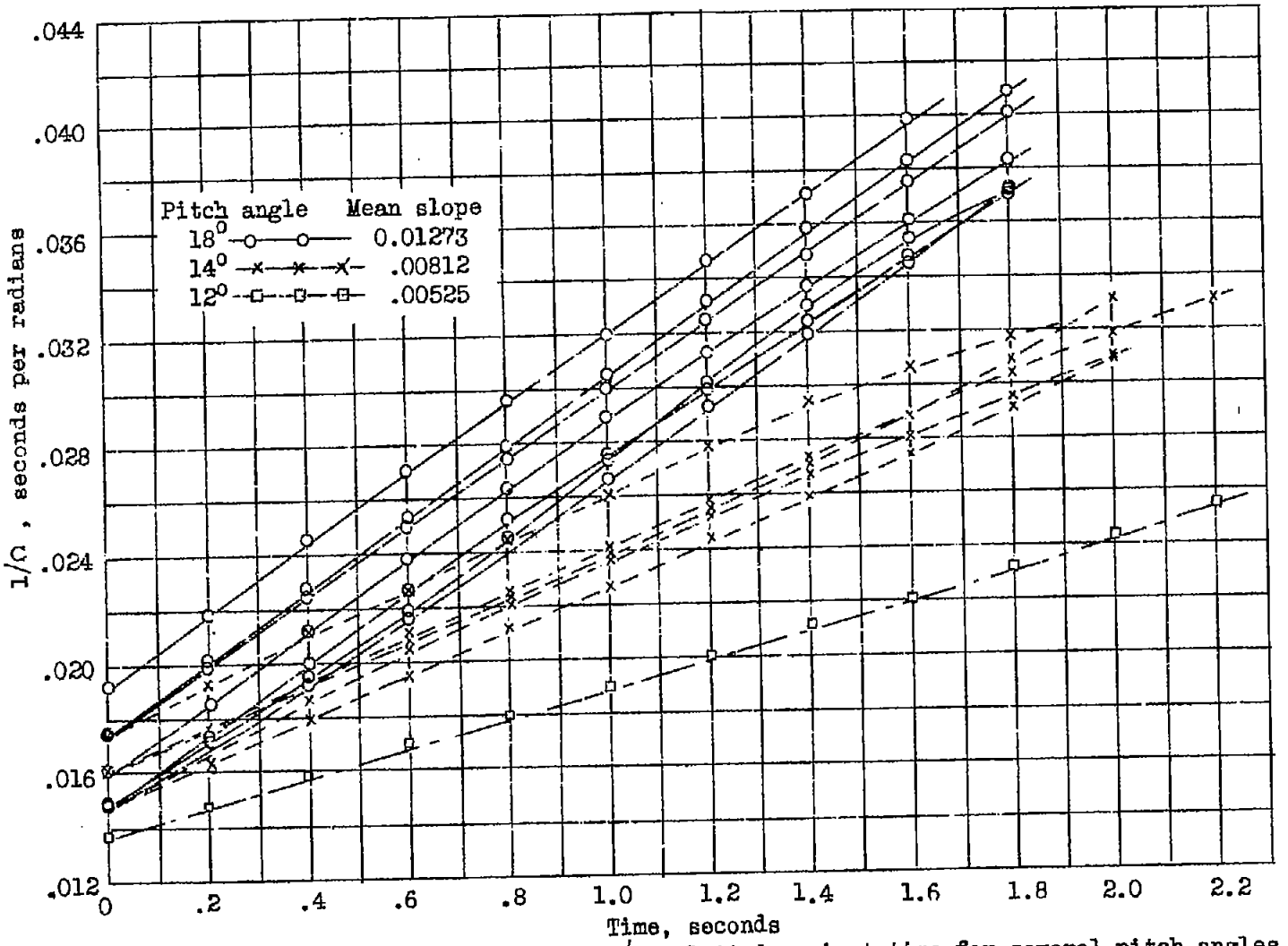

Figure 9.- Reciprocal of rotor speed, $1/\Omega$, plotted against time for several pitch angles and initial rotor speeds.

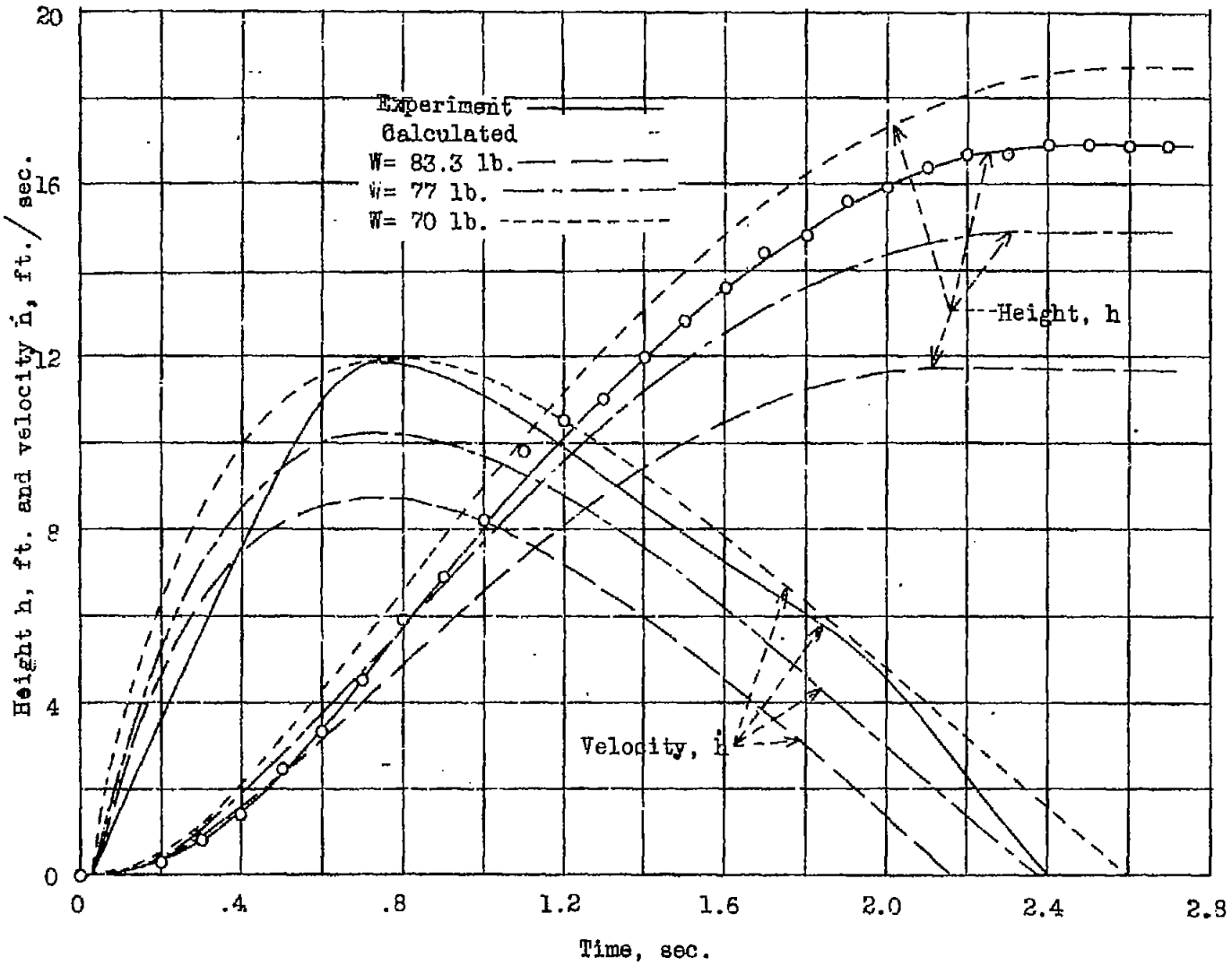

Figure 10.- Comparison of measured and calculated height and vertical velocity against time. W= 83.3 lb., θ_o= 10°, N_o= 700 r.p.m., T_c= 12.5 lb.

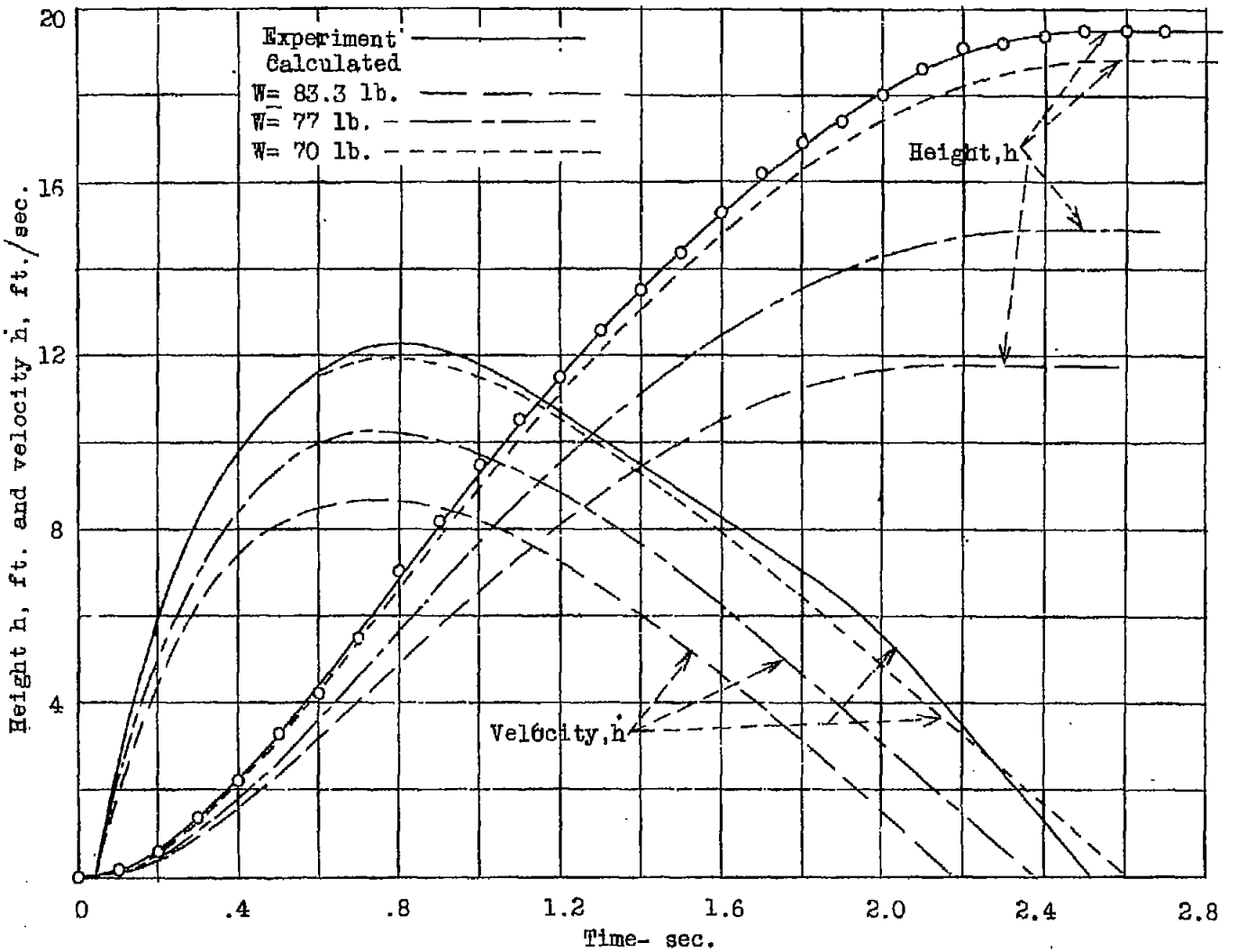

Figure 11.- comparison of measured and calculated height and vertical velocity against time. W = 83.3 lb, θ_o = 10°, N_o = 700 r.p.m., T_c = 17.5 lb.

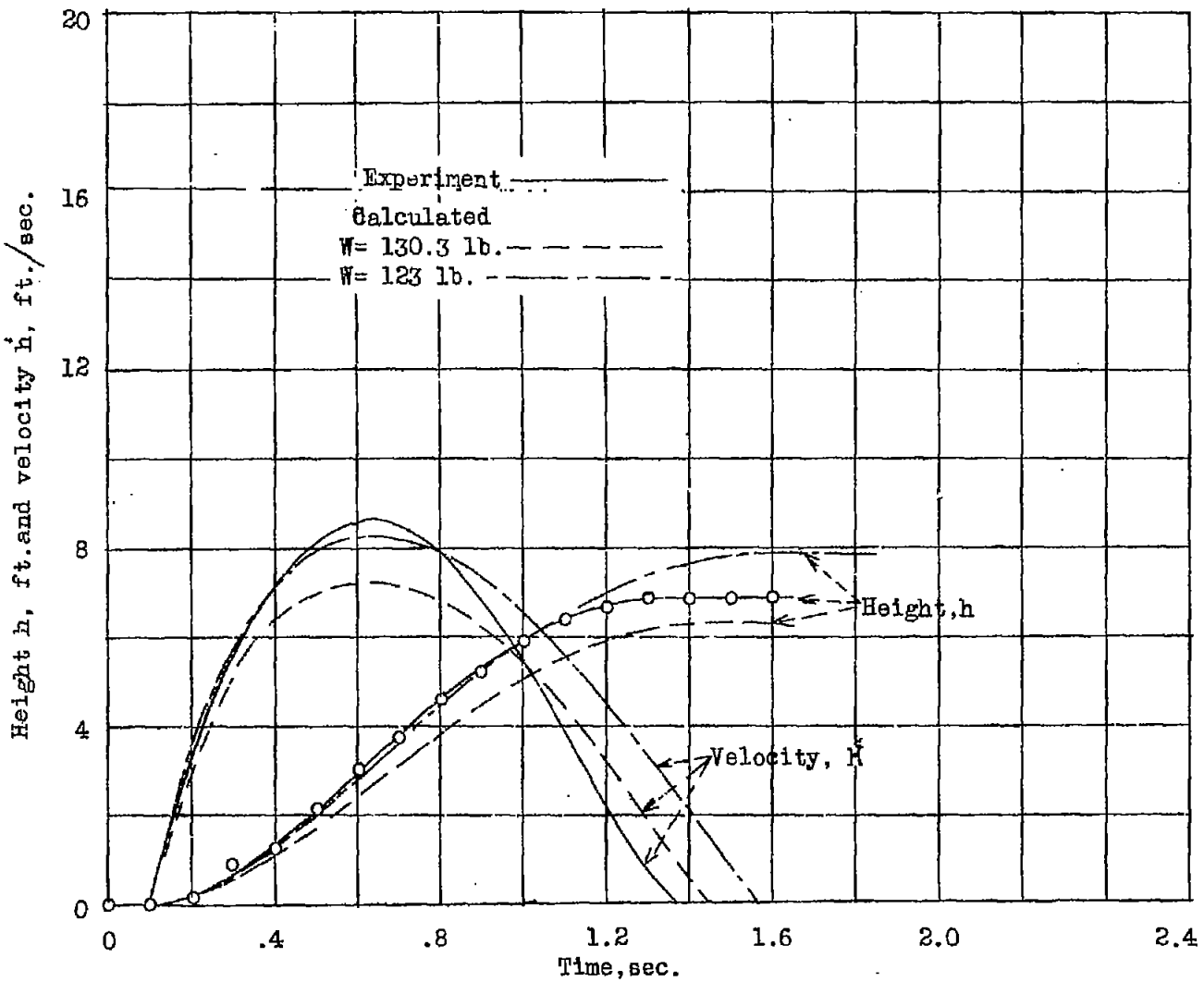

Figure 12.- Comparison of measured and calculated height and vertical velocity against time. W = 130.3 lb., $\theta_o = 18^o$, N_o = 600 r.p.m., T_c = 12.5 lb.